Progress in Organic Coatings 139 (2020) 105449

Contents lists available at ScienceDirect

Progress in Organic Coatings

journal homepage: www.elsevier.com/locate/porgcoat

Development of BPA-free anticorrosive epoxy coatings from agroindustrial waste

Lucas Renan Rocha da Silva[a], Francisco Avelino[b], Otilio Braulio Freire Diogenes[c], Vinicius de Oliveira Fidelis Sales[c], Kassia Teixeira da Silva[a], Walney Silva Araujo[c], Selma E. Mazzetto[a], Diego Lomonaco[a,*]

[a] Departament of Organic and Inorganic Chemistry, Federal University of Ceara, 60440-900, Fortaleza, CE, Brazil
[b] Federal Institute of Education, Science and Technology of Ceará, Iguatu, CE, 63503-790, Brazil
[c] Department of Metallurgical and Materials Engineering, Federal University of Ceara, 60440-900, Fortaleza, CE, Brazil

ARTICLE INFO

Keywords:
Agrowaste
BPA-free
Epoxy resin
Corrosion protection
Bio-based coatings

ABSTRACT

Epoxy resins are a versatile class of thermosetting precursors. The most commonly used compound in the production of these resins has been bisphenol A (BPA). However, due to its proven toxicity, one of the biggest challenges has been replacing BPA with renewable and non-toxic phenols. In this sense, novel epoxy coatings were prepared from the direct valorization of the cashew nutshell liquid (CNSL) as alternatives anticorrosive coatings for steel. The epoxy resin was obtained by epoxidation of double bonds in the aliphatic chain of cardanol and cardol using *in situ* performic acid generated by a solvent-free methodology. The chemical structure of the resin was evaluated by spectroscopic techniques such as FTIR and ^{1}H and ^{13}C NMR. For the coatings preparation, epoxidized-CNSL (e-CNSL) resin was cured with different curing agents (DETA, IPDA and PFDA) and the resultant thermosettings were analyzed regarding their chemical, thermal, mechanical and anticorrosive properties using the DGEBA/IPDA coating as reference. The anticorrosive properties of the coatings were evaluated by electrochemical impedance spectroscopy. The results showed that e-CNSL-based coatings have great potential as bio-based coatings for corrosion protection, being an interesting alternative to replace the current BPA-based materials.

1. Introduction

Many strategies to protect the metal against the corrosion process include the application of corrosion inhibitors, coatings (organic or inorganic) and the use of electrochemical protection (sacrificial anode, cathodic protection, etc.). Among these methods, organic coatings are widely used, acting as a physical barrier insulating metals from corrosive media, and can be applied as protection in the transport sectors in automobiles, airplanes, ships, etc, and also in engineering works such as pipes, bridges, buildings, etc. [1].

Epoxy resins are a very versatile class of thermosetting polymers widely used in a wide range of segments, such as adhesives, composites, building materials, laminates, insulation and especially coatings that domitate the market [2,3]. These resins account for about 70 % of the market for thermosetting materials [4] due to their adhesion properties, high chemical resistance, corrosion and moisture, excellent thermal stability, good mechanical properties and easy processability, which are suitable features for industrial and technological applications that require high performance [5].

In the development of anti-corrosive coatings, the epoxy resins can be cured with a wide variety of hardeners, such as polyfunctional amines, acids, anhydrides, phenols, alcohols and thiols to produce a three-dimensional reticulated network structure which acts as a barrier between the substrate and the environment to which it is exposed [6]. However, epoxy resins-based coatings are not perfect barriers, since they can absorb water, oxygen and ions, besides having low tenacity [7].

The synthesis of these resins involves a phenolic precursor derived from petrochemical derivatives, as they are able to confer high thermal and mechanical properties to the epoxy network [8]. Among these compounds, bisphenol A (BPA) is an aromatic monomer widely used in the manufacture of epoxy resins, such as the diglycidyl ether of bisphenol A (DGEBA), the most known produced and used type of BPA-based epoxy resin.

DGEBA has excellent thermal and mechanical performance properties as well as high chemical resistance, which are fundamental

* Corresponding author.
E-mail address: lomonaco@ufc.br (D. Lomonaco).

https://doi.org/10.1016/j.porgcoat.2019.105449
Received 21 July 2019; Received in revised form 11 November 2019; Accepted 19 November 2019
Available online 28 November 2019

features for protective coatings. However, recent studies have shown that BPA can cause extremely harmful effects on health and the environment by acting as an endocrine disruptor and a "carcinogenic, mutagenic and reprotoxic agent" (CMR). In addition, epichlorohydrin, a substance used in the production of DGEBA, is highly toxic and also a substance classified as CMR [9].

In this context, non-toxic and renewable materials have been studied as alternative that may reduce and/or replace the use of BPA and that can provide coatings with hydrophobicity and flexibility, improving the anticorrosive properties. Among promising and renewable resources, cashew nutshell liquid (CNSL) stands out as a low-cost and widely available agro-industrial waste.

CNSL is considered a versatile and valuable raw material for the production of thermally stable polymeric coatings, since its structure can be tailored through different chemical modifications to yield specific physicochemical properties. CNSL is composed of phenolic compounds with long unsaturated alkyl chains, making it a versatile platform for chemical modifications, representing a natural alternative to petrochemical derivatives.

CNSL is obtained as a byprodutct from the cashew nutshell (*Anacardium occidentale* L.) during its industrial processing. This agroindustrial residue represents around 25 % of the cashew nut weight and, after the industrial thermal treatment, its composition is basically of cardanol (65–75 %) and cardol (10–20 %) being produced as a low-added value agroindustrial byproduct [10,11].

The constituents of CNSL present in their structures three reactive sites: phenolic hydroxyls, aromatic ring and a long unsaturated side-chain [10]. The presence of the long side chain along with a phenolic core gives CNSL interesting properties such as adhesion to various substrates, chemical and thermal resistance, anticorrosive properties and surfactant effect, making it a versatile platform for various chemical modifications according to the application needs.

The main component of the CNSL, cardanol, has been already studied for applications in the synthesis of bio-based materials, as plasticizer for PVC [12], polyurethanes coatings [13], curing agent for epoxy resins [6], flame retardants [9], nanocomposite for corrosion protection [14] and the partial or total substitution of phenol in thermosettings, such as phenolic resins [15].

Based on the above, the direct use of CNSL, without prior separation of its components, is an excellent alternative to petroleum-based coating materials, which is still not well explored in the scientific literature. Therefore, the aim of this work was promote the direct valorization of CNSL for epoxy resin production, totally replacing BPA, by using eco-friendly methodology, for the subsequent evaluation of its potential as anticorrosive protective coating for steel surfaces.

2. Materials and methods

2.1. Materials

Cashew nutshell liquid (CNSL) was supplied by Amêndoas do Brasil LTDA (Fortaleza-CE, Brazil). All reagents were used as received: sodium bicarbonate (Synth), Hydrogen peroxide (35 %, Synth), acetone (Synth), ethyl acetate (Synth), formic acid (85 %, Dinâmica), diglycidyl ether of bisphenol A (DGEBA) (Avipol), *p*-phenylenediamine (99 %, Sigma), sodium sulfate (99 %, Sigma), isophorone diamine (IPDA) (99 %, Sigma), diethylenetriamine (99 %, Sigma), crystal violet (for microscopy, Sigma), 33 % wt. hydrobromic acid in acetic acid (Sigma), and Celite® S (99 %, Sigma).

2.2. Epoxidation of CNSL

The epoxidation of double bonds of CNSL was performed according to the methodology described by Moreira et al. [16] with some modifications (Fig. 1).

CNSL (10.00 g) and formic acid (3.60 g, 0.066 mol) were mixed in a 150 mL flask and stirred at room temperature. Then, 35 % v/v H_2O_2 (19.10 mL, 0.222 mol) was added dropwise over 30 min. At the end of the addition, the mixture was held at 65 °C for 1 h under magnetic stirring. After the reaction was completed, the crude product was purified by solvent extraction (100 mL of ethyl acetate) and neutralized with saturated sodium bicarbonate solution (2 × 20 mL). The organic phase was collected, dried using anhydrous sodium sulfate and concentrated under reduced pressure, obtaining 9.0 g of a reddish-brown viscous liquid (yield: 90 % in relation to cardanol and cardol present in the CNSL).

2.3. Preparation of test specimens

Preparation of test specimens was performed based on the epoxy content (EC, mmol g^{-1}) of e-CNSL and DGEBA and the amount of reactive hydrogens in each amine (DETA, IPDA and PFDA). 3.0 g of resin with the respective amine in a ratio of 5:1 or 4:1 (mol of epoxy/mol of amine) were mixed. Thus, the calculated amount of curing agent and epoxy resin were mixed with acetone and were poured into a Teflon mold and subjected to a vacuum degassing for 10 min to remove the remaining air bubbles. The specimens were allowed to dry for 18 h and then subjected to a controlled temperature program: 60, 80, 100 °C for

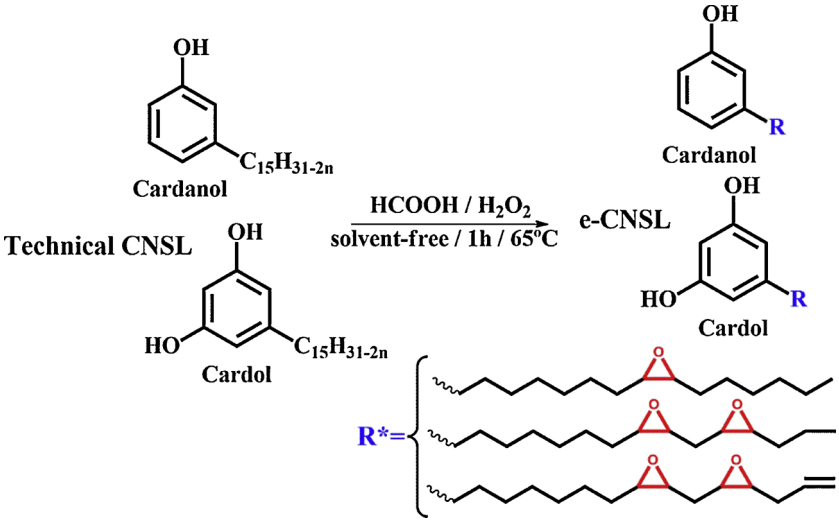

Fig. 1. Solvent-free epoxidation reaction through the in situ performic acid generation.

1 h and 130 °C for 2 h. The specimens were submitted to a post curing process at 150 °C for 2 h.

2.4. Surface preparation

1010 steel panels (10 cm x 15 cm) had their surfaces treated by steel shot blasting followed by cleaning with acetone prior to resin application. The panels had roughness of 50 μm and were measured by PosiTector®SPG equipment.

2.5. Application and curing of coatings

Coatings were prepared to evaluate the adhesive and anticorrosive properties. Coating solutions with e-CNSL/DETA, e-CNSL/IPDA, e-CNSL/PFDA and DGEBA/IPDA were prepared using methyl ethyl ketone (MEK) as solvent to achieve the viscosity required for application. These solutions were then applied to steel metal substrates by conventional air spray gun. The coated substrates were allowed to dry for 18 h and then placed in an oven and subjected to the same temperature controlled program as described in section 2.3. The coated panels were conditioned at room temperature for 24 h prior to testing.

2.6. Characterization techniques and test methods

2.6.1. Characterization of CNSL and liquid epoxy resin

The iodine value was calculated according to ASTM D1959 with modifications [17]. The epoxy equivalent weight (EEW) of the e-CNSL and DGEBA resins were determined by the volumetric titration method. The known weight of the sample was completely dissolved in 50 mL of ethyl acetate. It was then titrated with 0.1 N HBr solution using crystal violet (1 mg mL^{-1} in acetic acid) as colorimetric indicator. The determination was performed in triplicate for each sample. The EEW of the resin was calculated using Eq. (1):

$$EEW\left(\frac{g}{eq}\right) = \frac{43x100}{E} \quad (1)$$

where 43 = molar weight of the epoxy ring.

Epoxide Content (EC) is calculated according to Eq. 2:

$$EC\left(\frac{mmol}{g}\right) = \frac{(VxN)}{M} \quad (2)$$

Where V is the volume of HBr used to titrate the sample in mL, N is the normality of the HBr solution in mol L^{-1}, and W is the mass of the sample in g.

The CNSL and e-CNSL were characterized by the presence of functional groups by Fourier Transform Infrared Spectroscopy (FTIR) performed on a Perkin Elmer FT-IR/NIR FRONTIER using an attenuated total reflectance (ATR) accessory with zinc selenide crystal (ZnSe). The spectra were acquired with 32 scans between 4000 and 550 cm^{-1} with 4 cm^{-1} resolution.

The chemical structure of e-CNSL resin was further confirmed by NMR analysis carried out in a Bruker Avance DPX 300 spectrometer operating at 300 and 75 MHz for the ^{1}H and ^{13}C nuclei, respectively, at room temperature using deuterated chloroform ($CDCl_3$) as solvent. The e-CNSL (30 mg) was dissolved in 0.4 mL of $CDCl_3$-d and the residual solvent signal was used as the internal reference (7.27 and 77.3 ppm, for ^{1}H and ^{13}C, respectively). The signals were assigned taking into account previous descriptions of chemical changes as already mentioned in the literature [18].

2.6.2. Properties of the test specimens

The gel content (GC) of the cured films was determined by gravimetric analysis according to ASTM D2765 with modifications [19]. Samples of the cured films (Wi) were immersed in 3 mL of THF for 24 h to extract the soluble contents. After this period, the samples were dried at room temperature until a constant weight (Wf). The analysis was performed in triplicate, and the GC of the samples were calculated by Eq. 3:

$$GC(\%) = \frac{Wf}{Wi}x100 \quad (3)$$

These values express in percent the non-soluble gel content which can be correlated with a crosslink density formed in the polymers.

The contact angle measurement of the cured specimens was determined using a WCA instrument (GBX Instrumentation Scientification). The images were recorded using a camera (Nikon PixeLINK) coupled to the WCA equipment for short periods of time. For each polymer, three specimens were used for analysis.

2.6.3. Thermogravimetric analysis

The thermal behavior of the cured coatings was studied by thermogravimetric analysis (TGA, Mettler-Toledo TGA/SDTA851e). For the TGA analysis, 5 mg of sample were heated from 30 to 800 °C under N_2 atmosphere and from 30 to 600 °C under synthetic air atmosphere (50 mL min^{-1}) at a rate of 10 °C min^{-1}.

2.6.4. Differential scanning calorimeter

For the polymerization study the samples were evaluated by differential scanning calorimetry (DSC, Mettler-Toledo DSC 823e) by heating from 30 °C to 400 °C at a heating rate of 10 °C min^{-1}. For the evaluation of the glass transition temperature (T_g) of the polymers, 5 mg of sample were heated from 30 to 150 °C, cooled from 150 to -30 °C and heated at -30 to 150 °C under a nitrogen atmosphere (50 mL min-1) at a heating rate of 20 °C min^{-1}.

2.6.5. Adhesive and anticorrosive properties of coatings

The thickness of the coatings were measured with PosiTector® 6000 equipment. The coatings were tested for pull-off adhesion properties using the PosiTest AT-A test apparatus according to ASTM D4541-17 (Test Method E) [20]. For the accomplishment of the test of adhesion an aluminum pin was glued on the surface of the cured coating with epoxy glue with drying period of 24 h. The strength adhesion was recorded after the detachment between the coating and the substrate. The adhesion tests were performed three times to verify the repeatability of the measurements.

The corrosion resistance properties of the cured coatings were evaluated using an electrochemical impedance spectroscopy (EIS) study on the potentiostat AUTOLAB PGSTAT302 P. A conventional three-electrode system was used, in which the silver/silver chloride electrode, platinum electrode and the coated panels were used as reference, counter and working electrodes, respectively. The surface area of the working electrode exposed to the test solution (3.5 % in m / v NaCl) was 5.07 cm^2 in all cases at a temperature of 22 °C. The frequency range used was 1×10^5 - 6×10^{-3} Hz with an amplitude of 25 mV.

3. Results and discussion

3.1. Characterization of e-CNSL

3.1.1. Chemical characterization

The structure of e-CNSL resin was evaluated by chemical and spectroscopic analyses. The chemical characterization includes the determination of the iodine value and epoxy content in the resin and the results are expressed in Table 1. As can be seen in Table 1, the iodine

Table 1
Chemical characterization of e-CNSL resin.

Sample	Iodine value (g/100 g)	Epoxy content (mmol/g)	EEW (g/eq)
CNSL	169	–	–
e-CNSL	64	2.13	469
DGEBA	–	5.41	190

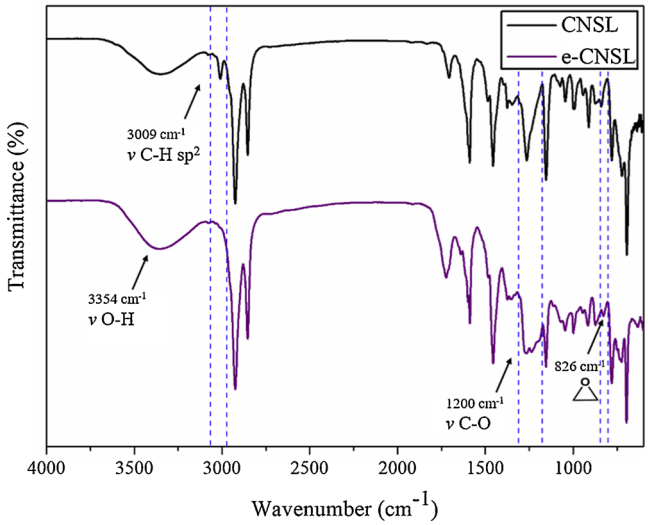

Fig. 2. FTIR spectra of CNSL and e-CNSL.

value of e-CNSL resin decreased in relation to that of CNSL, confirming the conversion of the double unsaturations in the aliphatic chains of cardanol and cardol into oxirane groups by the epoxidation reaction.

The notorious differences between the epoxy content values of e-CNSL and DGEBA, Table 1, can be explained by the different mechanisms involved in each resin synthesis. For DGEBA, the glycidylation reaction occurs in both phenolic hydroxyls, while for e-CNSL the epoxidation only occurs on the double bonds, which decrease the number of oxirane groups per mass of resin.

3.1.2. Spectroscopic measurements

Through FTIR analysis it was possible to investigate structural modifications occurred during the epoxidation reaction through the disappearance and appearance of characteristic absorption bands related to the structure of CNSL and e-CNSL, as shown in Fig. 2.

In the CNSL spectrum, a broad band related to the phenolic hydroxyl group is observed at 3354 cm^{-1}; C–H stretching for the unsaturated side chain of the CNSL constituents at 3009 cm^{-1}, as well as C–H stretching for the methyl, methylene and methine groups at 2924, 2853 and 1456 cm^{-1}; C═C stretching of the aromatic ring (1595 cm^{-1}). In the e-CNSL spectrum, observed the symmetrical stretching C–O (1200 cm^{-1}), the appearance of the asymmetric stretching band of the epoxy ring (826 cm^{-1}) and the disappearance of the band at 3009 cm^{-1} (C–H stretching from the inner unsaturated side chain of the CNSL constituents) completely after epoxidation due to the conversion of double bonds to epoxy groups. Similar results were as also observed by LIU and collaborators [18].

Figs. 3 and 4 show the ^{1}H and ^{13}C NMR spectra of CNSL and e-CNSL, respectively, in which their main structural modifications can be identified and used as evidences of the successful formation of the oxirane rings [18,21].

The characteristic signals ranging from 6.0–7.5 ppm (aromatic protons **a**, **a'**, **c** and **b**) are related to the protons of cardanol and cardol aromatic ring.

Comparing the CNSL and e-CNSL spectra, the peaks in the range of 5.3–5.5 ppm (internal double bond protons **m** and **n**) relative to the hydrogen of the internal double bonds of the C_{15} chain almost disappeared. This indicates the conversion of the internal double bonds of the side chain into epoxy groups during the epoxidation reaction. Moreover, new signals appeared between 2.9 and 3.2 ppm (protons **h**), which are assigned to the hydrogens of the oxirane ring, indicating the successful formation of epoxy groups. In addition, the displacement of the chemical shifts of the peaks in the range of 1.3–1.7 ppm (protons **e** and **f**) also supports the formation of epoxy groups.

However, there were no significant changes in the peaks ranging from 5.8 to 5.9 ppm and from 5.0–5.1 ppm, which are the protons related to the terminal double bonds of the chain. This shows that the terminal double bonds were not epoxidized. As a matter of fact, since the methodology used was the Prilezhaev reaction and as the synthesis of e-CNSL was performed without solvent (heterogeneous system), the high rate of formation and consumption of the performic acid makes it possible only the epoxidation of more reactive alkenes (substituted), less substituted alkenes present low reactivity for this type of epoxidation, as is the case of the terminal unsaturations of the cardanol and cardol chains [4].

In Fig. 4(a), the ^{13}C NMR spectrum shows peaks in the range of 114.7 and 137.1 ppm, in which some of them have disappeared, as shown in Fig. 4(b). Likewise, the epoxy groups differed between CNSL and e-CNSL with the appearance of new peaks between 54.45 ppm and 57.61 ppm corresponding to the carbons present in the oxirane ring.

3.2. Study of polymerization of e-CNSL resin with cure agents

The thermal behavior of e-CNSL with amine hardeners (DETA, IPDA and PFDA) was studied by differential scanning calorimetry (DSC) and the DGEBA with IPDA commercial epoxy resin was compared. The exothermic curves related to oxirane ring-opening polymerization are shown in Fig. 5, while the initial polymerization temperature (T_{onset}) and the maximum polymerization temperature (T_{max}) are summarized in Table 2.

The exothermic peak in neat e-CNSL thermogram can be attributed to oxirane rings opening reactions by phenolic hydroxyl groups of cardanol and cardol. In the e-CNSL/DETA, e-CNSL/IPDA and e-CNSL/PFDA formulations, the exothermic event is caused by the oxirane ring opening reaction through an S_N2 mechanism involving a nucleophilic attack of an amino group to one of the carbon atoms of the epoxide.

Compared to neat e-CNSL, the use of amine curing agents significantly decreased the initial polymerization temperature (T_{onset}) in all formulations. The order of nucleophilic reactivity of the amines in the three formulations according to T_{max} were e-CNSL/PFDA < e-CNSL/IPDA < e-CNSL/DETA. As expected, aliphatic amines increased the cure rate in the polymerization reactions, however, IPDA being a branched amine with considerable steric hindrance, presented a broad polymerization curve [22].

3.3. Characterization of the specimens

3.3.1. Spectroscopic measurements

The fully cured specimens were analysed by FTIR in order to assess any functional group conversion, as shown in Fig. S1. It was observed the occurrence of a C═C stretching of the aromatic ring of the *p*-phenylenediamine in 1516 cm^{-1} in the spectrum e-CNSL / PFDA, and the appearance at 822 cm^{-1} from C–H out-of-plane bending band in spectra of aromatic 1,4-disubstituted ring [23–25]. In all spectra of polymers is an average intensity and broad band at 1065 cm^{-1} due to a C–N stretch. In the e-CNSL/DETA and e-CNSL/IPDA spectra are observed the disappearance of the band at 826 cm^{-1} related to the oxirane group, indicating the epoxy ring opening reaction by the amine hardeners [26].

3.3.2. Gel content (GC)

The gel content of the cured specimens was measured in order to assess the extent of curing of the four formulations. In Table 3 are summarized the results obtained. The average gel content for all formulations derived from e-CNSL was found to be in the range of 70–80 %, as shown in Table 3, indicating that the network contains uncrosslinked chains, such as non-functionalized cardanol chains, or are saturated, which can increase the soluble parts and consequently decrease the GC.

In fact, the use of different curing agents also makes it possible to

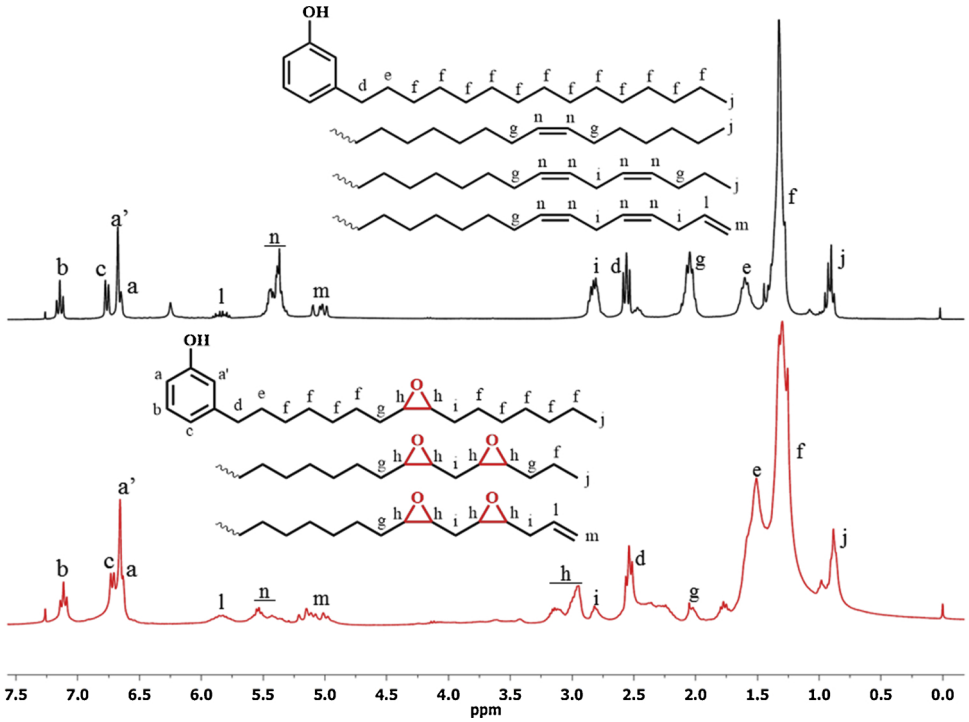

Fig. 3. ^{1}H NMR spectra of CNSL and e-CNSL.

obtain materials with different GC values at the same temperature. This is caused by the chemical structure of these curing agents. DETA is the most reactive because of its aliphatic and polyfunctional nature promoting highly interconnected networks. In the case of PFDA, an aromatic and less nucleophilic amines, the curing reaction occured slower than that of DETA and IPDA. For the case of IPDA, its lower reactivity compared to DETA may be related to its steric hindrance caused, resulting in a less crosslinked network.

3.3.3. *Contact angle*

Fig. 6 shows the test performed with water on coatings derived from e-CNSL illustrating their hydrophobic properties. The contact angles of the e-CNSL/IPDA, e-CNSL/DETA, e-CNSL/PFDA coatings are summarized in Table 3. In general, the hydrophilic properties of the epoxy may be due to the hydrophilic groups present in the polymer, mainly secondary amine groups formed during the epoxy opening reaction [27]. The highest contact angle value was observed in the e-CNSL / PFDA formulation, where an aromatic amine was used, which provided the

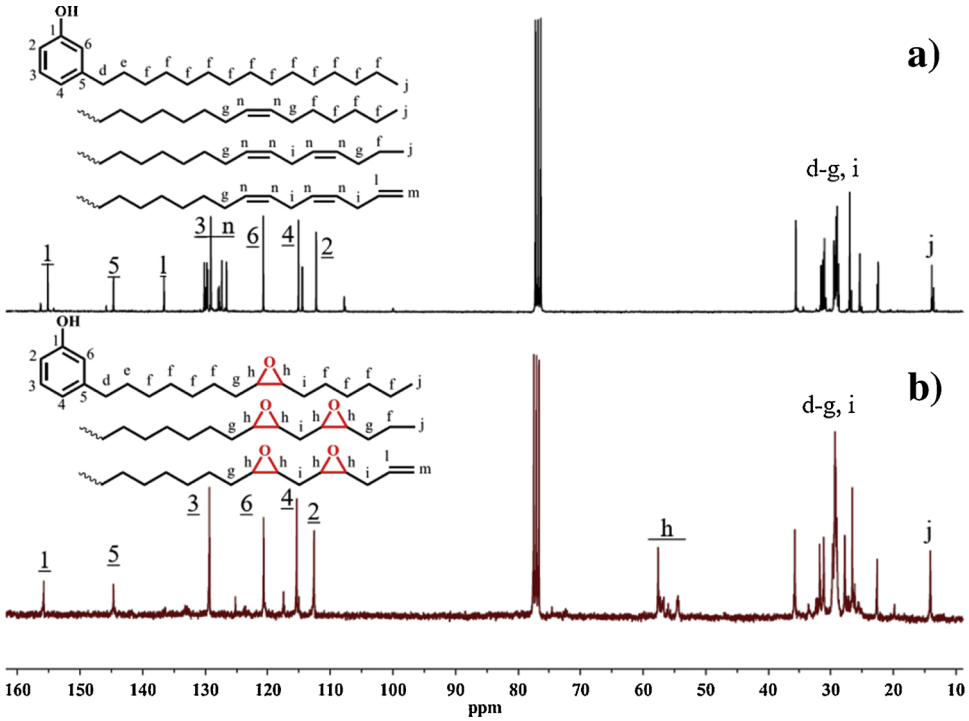

Fig. 4. ^{13}C NMR spectra of (a) CNSL and (b) e-CNSL.

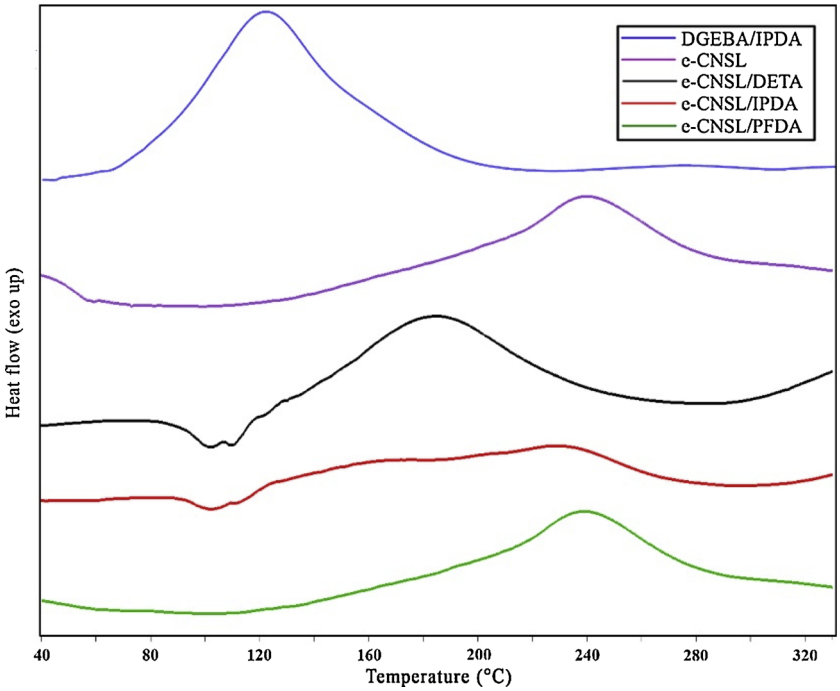

Fig. 5. Polymerization of DGEBA resin with IPDA and e-CNSL epoxy resin with DETA, IPDA and PFDA amines.

Table 2
T_{onset} and T_{max} temperatures of epoxy resins polymerization.

Samples	Temperature (°C)	
	T_{onset}	T_{max}
DGEBA	68	111
e-CNSL	123	239
e-CNSL/DETA	109	185
e-CNSL/IPDA	109	229
e-CNSL/PFDA	116	239

Table 3
Gel content, contact angle, thermal and mechanical properties of e-CNSL coatings.

Sample Name	e-CNSL/DETA	e-CNSL/IPDA	e-CNSL/PFDA
Gel content (%)	82	70	72
Contact angle (°)	72,7	76,9	87,6
T_g (°C)	12	15	18
T_{onset} (°C)	292 (N_2) / 277 (air)	297 (N_2) / 281 (air)	282 (N_2) / 276 (air)
$T_{d30\%}$ (°C)	393 (N_2) / 406 (air)	367 (N_2) / 399 (air)	397 (N_2) / 412 (air)
$T_{d50\%}$ (°C)	428 (N_2) / 435 (air)	418 (N_2) / 433 (air)	434 (N_2) / 443 (air)
Adhesion *Pull Off* (MPa)	10	10,2	9,8

material with greater hydrophobicity, possibly due to the presence of aromatic amine groups, which electrons pair is in resonance with the benzene ring, making them less available for interaction with water molecules through hydrogen bonds. The contact angle values changed according to the curing agents used were: aliphatic < cycloaliphatic < aromatic amines.

3.4. Thermal properties

3.4.1. Glass transition temperature

The glass transition temperatures (T_g) of all coatings were determined by DSC analysis and are shown in Fig. S2 and the values in Table 3. The glass transition temperature values of the e-CNSL derived coatings can be attributed to the presence of the aliphatic chain of cardanol and cardol which can impart a plasticizing effect to the structure of the polymers [6]. In addition, it can be seen that the chemical structure of the curing agents used also affects the T_g of the materials. Curing agents such as linear aliphatic amines favor the reduction of T_g, since they increase the distance between the polymer chains, while cycloaliphatic and aromatic amines tend to increase the T_g values giving the materials greater rigidity to their structure.

3.4.2. Thermogravimetric analysis

TGA analysis was performed for cured polymers to investigate the thermal stability of materials under different atmospheric conditions (inert and oxidative atmosphere) and the results are summarized in

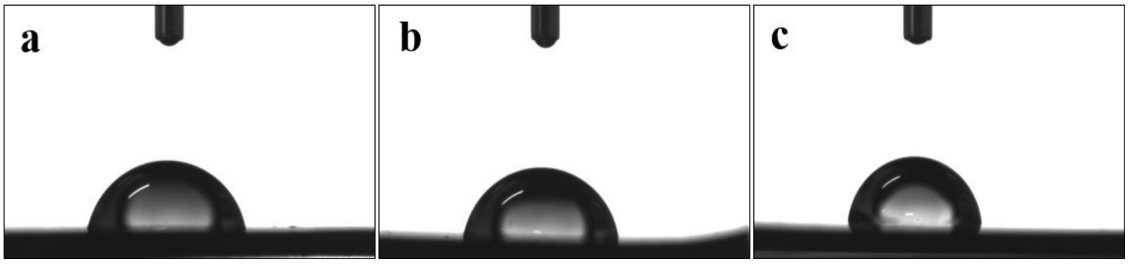

Fig. 6. Contact angle of the specimens: a) e-CNSL/DETA; b) e-CNSL/IPDA and c) e-CNSL/PFDA.

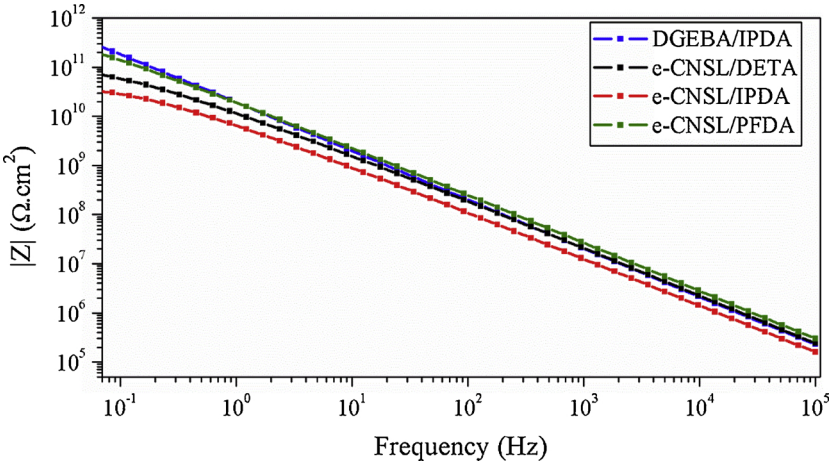

Fig. 7. Bode plots of coatings cured with amines.

Table 3. All polymers derived from e-CNSL were similar under inert atmosphere, showing initial degradation temperatures (T_{onset}) in the range of 280 − 300 °C.

Under oxidative atmosphere the coatings also presented similar T_{onset} around 280 °C. It is interesting to note that the aromatic ring of the PFDA ensured the material a very good thermal resistance of 412 °C in $T_{30\%}$ and 443 °C in $T_{50\%}$.

3.5. Corrosion resistance property

3.5.1. Measurement of electrochemical impedance spectroscopy (EIS)

Electrochemical impedance spectroscopy (EIS) was performed to evaluate the anticorrosive potential of the bio-based coatings on the 1010 steel surface (Fig. S3). For comparison purpose, a standard coating, made from DGEBA and IPDA, was also prepared. The thicknesses of all coatings were measured in the range of 160 − 180 μm. As the organic coatings act as a physical barrier between solution and substrate, a perfect combination of factors, including the hydrophobicity of reagents used in the preparation of coatings and the high crosslink density, is required to achieve a perfect barrier [28].

From the Bode module and phase angle plots (Fig. 7 and Fig. S4) it is possible to obtain informations about the response of the impedance at high frequency regions (on the electrolyte resistance) and low frequency (relative to the coating resistance) during the immersion period of the coatings in the solution. The high impedance modulus value at low frequencies and the occurrence of a single half-circle on the Nyquist plot (Fig. 8), indicating the presence of only one time constant, showing that the coating acted as a barrier, promoting effective metal protection [7].

The values of coating resistence (R_C) at a given time brings information about the state of degradation of the paint, when this value is grater than 10^6, the paint is viewed as being a good organic coating [29]. This study revealed that all coatings presentend values of R_C higher than 10^6 (Table 4), showing that all of them can be considered as being a good organic coating. The commercial coating (DGEBA/IPDA) showed to be highly capacitive, acting as a perfect capacitor profile, with high impedance values as showed in Fig. 8. The coatings cured with different amine curing agents (aliphatic, cycloaliphatic and aromatic) provided different properties for corrosion resistance. In this preliminary study, e-CNSL/PFDA was the most effective among the bio-based coatings developed, providing the corrosion protection of the steel under a NaCl solution environment. The elevated impedance value can be associated to its high hydrophobicity, as previously observed by

Table 4
Corrosion parameter of coatings cured with DETA, IPDA and PFDA by EIS measurement.

Coating	Coating Resistance (ohm. cm^2)
DGEBA/IPDA	6.2×10^{12}
e-CNSL/DETA	1.1×10^{11}
e-CNSL/IPDA	4.1×10^{10}
e-CNSL/PFDA	1.0×10^{12}

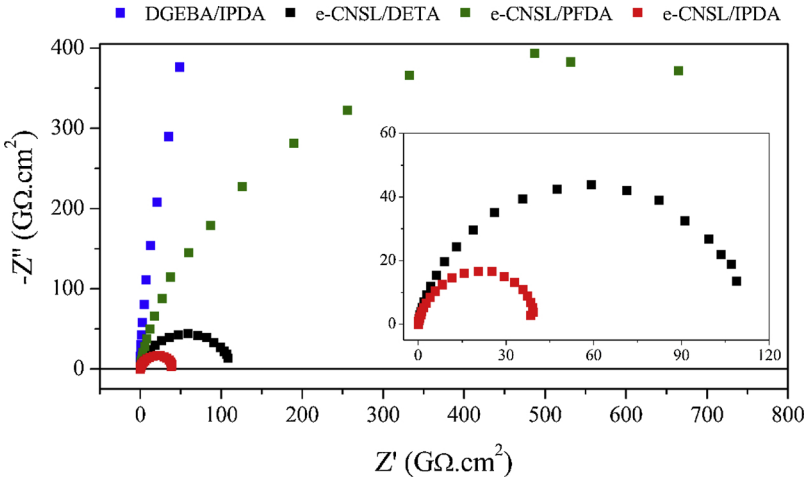

Fig. 8. Nyquist plot of coatings cured with amines.

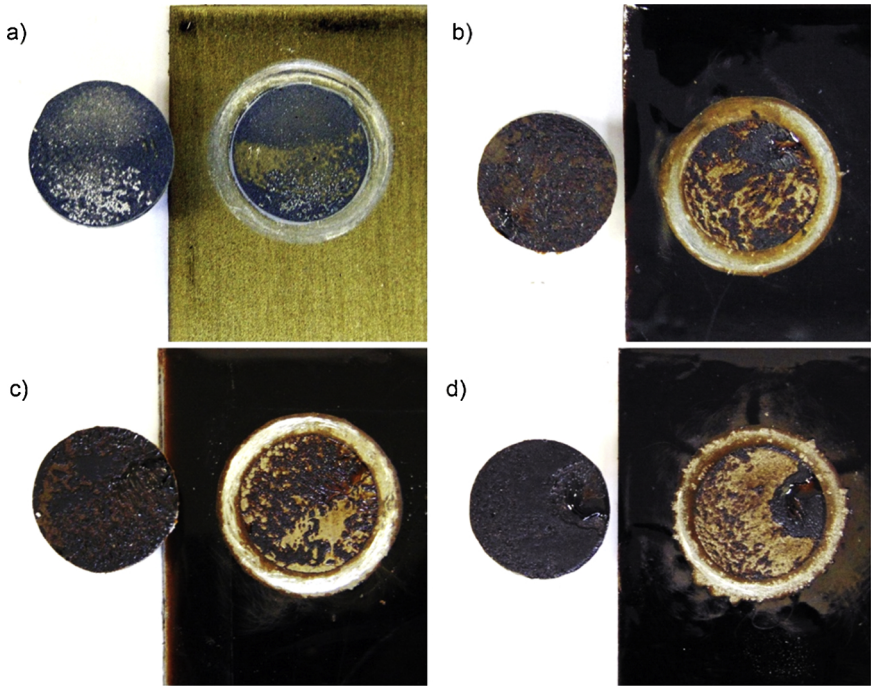

Fig. 9. The different epoxy coating panels after pull off adhesion tests: a) DGEBA/IPDA; b) e-CNSL/DETA; c) e-CNSL/IPDA e d) e-CNSL/PFDA.

contact angle analysis. However, the e-CNSL/IPDA coating presented the lowest impedance modulus in low frequency regions, indicating a higher penetration of the NaCl solution in this coating [30].

3.6. Adhesion test

The adherence of the developed coatings was analyzed by means of the pull-off adhesion test. The result of this test is given by the applied force and the type of failure that can be observed, being of two types: cohesive and adhesive. The adhesion strength of the coatings results are summarized in Table 3, while the failures test images are shown in Fig. 9. The commercial coating (DGEBA/IPDA) showed the highest adhesion value (12 MPa). Coatings derived from e-CNSL also showed very good adhesion values (~ 10 MPa). One of the main reasons for the high adhesion resistance in epoxy coatings is the presence of hydrogen bonds at the metal/epoxy interface [31].

In the epoxy resins, hydroxyl groups are responsible for this type of interaction. The higher the degree of cure, the greater the amount of hydroxyl groups formed and the greater the strength of adhesion.

In Fig. 9, it is possible to evaluate the type of failure caused by pulling the glued pins from the coatings surface. In Fig. 9a, it was observed that the glue adhered to the surface of the coating and there was no peeling/coating, only pine/glue. The e-CNSL coatings presented the two types of failure: cohesive and adhesive. The e-CNSL/DETA and e-CNSL/IPDA coatings showed cohesive failure, while the e-CNSL/PFDA and commercial (DGEBA/IPDA) coatings presented cohesive/adhesive failure.

Adhesive failure indicates a definitive separation between the coating and the metal substrate, while cohesive failure results when the adhesion at the interface exceeds the cohesion of the paint layer. The existence of this type of failure indicates the achievement of an optimal adhesion force.

4. Conclusion

Highly bio-based epoxy coatings were successfully developed from the agro-industrial waste CNSL, under simple and effective eco-friendly methodology. The coatings e-CNSL/DETA, e-CNSL/IPDA and e-CNSL/PFDA were evaluated as sustainable alternatives to replace/reduce the use of BPA-based epoxy resins in the field of anticorrosive organic coatings for the protection of steel surfaces. Due to the chemical composition of CNSL, combining a phenolic core with a lipidic side chain, the bio-based coatings presented a very good balance between flexibility and wettability properties along with excellent chemical resistance, thermal stability and anti-corrosion performance, indicating that these coatings can be considered promising sustainable anticorrosive solutions for the protection of metal substrates.

The authors declare the following financial interests/personal relationships which may be considered as potential competing interests:

Declaration of Competing Interest

The authors declare that they have no known competing financial interests or personal relationships that could have appeared to influence the work reported in this paper.

Acknowledgements

This study was financed in part by the Coordenação de Aperfeiçoamento de Pessoal de Nível Superior - Brasil (CAPES) - Finance Code 001; Conselho Nacional de Desenvolvimento Científico e Tecnológico (CNPq) (Grants # 407291/2018-0 and 409814/2016-4) and Fundação Cearense de Apoio ao Desenvolvimento Científico e Tecnológico (Funcap). The authors thank CENAUREMN (Centro Nordestino de Aplicação da Ressonância Magnética Nuclear at Fortaleza, Brazil) for the NMR analyses. We also thank Amêndoas do Brasil LTDA for the CNSL samples.

Appendix A. Supplementary data

Supplementary material related to this article can be found, in the online version, at doi:https://doi.org/10.1016/j.porgcoat.2019.105449.

References

[1] S.B. Lyon, R. Bingham, D.J. Mills, Advances in corrosion protection by organic coatings: what we know and what we would like to know, Prog. Org. Coat. 102 (2017) 2–7, https://doi.org/10.1016/j.porgcoat.2016.04.030.

[2] F. Ng, G. Couture, C. Philippe, B. Boutevin, S. Caillol, Bio-based aromatic epoxy monomers for thermoset materials, Molecules 22 (2017), https://doi.org/10.3390/molecules22010149.

[3] S. Kumar, S. Krishnan, S. Mohanty, S.K. Nayak, Synthesis and characterization of petroleum and biobased epoxy resins: a review, Polym. Int. 67 (2018) 815–839, https://doi.org/10.1002/pi.5575.

[4] G. Couture, L. Granado, F. Fanget, B. Boutevin, S. Caillol, Limonene-based epoxy: anhydride thermoset reaction study, Molecules 23 (2018) 2739, https://doi.org/10.3390/molecules23112739.

[5] P. Kasemsiri, A. Neramittagapong, P. Chindaprasirt, Curing kinetic, thermal and adhesive properties of epoxy resin cured with cashew nut shell liquid, Thermochim. Acta 600 (2015) 20–27, https://doi.org/10.1016/j.tca.2014.11.031.

[6] K. Wazarkar, A. Sabnis, Cardanol based anhydride curing agent for epoxy coatings, Prog. Org. Coat. 118 (2018) 9–21, https://doi.org/10.1016/j.porgcoat.2018.01.018.

[7] J. Lv, Z. Liu, J. Zhang, J. Huo, Y. Yu, Bio-based episulfide composed of cardanol/cardol for anti-corrosion coating applications, Polymer (Guildf.) 121 (2017) 286–296, https://doi.org/10.1016/j.polymer.2017.06.036.

[8] C.O. Tuck, E. Pérez, I.T. Horváth, R.A. Sheldon, M. Poliakoff, Valorization of biomass: deriving more value from waste, Science (80-) 337 (2012) 695–699, https://doi.org/10.1126/science.1218930.

[9] Y. Ecochard, M. Decostanzi, C. Negrell, R. Sonnier, S. Caillol, Cardanol and eugenol based flame retardant epoxy monomers for thermostable networks, Molecules 24 (2019) 1–21, https://doi.org/10.3390/molecules24091818.

[10] D. Lomonaco, G. Mele, S.E. Mazzetto, Cashew nutshell liquid (CNSL): from an agro-industrial waste to a sustainable alternative to petrochemical resources, Cashew Nut Shell Liq. A Goldf. Funct. Mater. (2017), https://doi.org/10.1007/978-3-319-47455-7_2.

[11] J. Mgaya, G.B. Shombe, S.C. Masikane, S. Mlowe, E.B. Mubofu, N. Revaprasadu, Cashew nut shell: a potential bio-resource for the production of bio-sourced chemicals, materials and fuels, Green Chem. 21 (2019) 1186–1201, https://doi.org/10.1039/c8gc02972e.

[12] B. Briou, S. Caillol, J.J. Robin, V. Lapinte, Non-endocrine disruptor effect for cardanol based plasticizer, Ind. Crops Prod. 130 (2019) 1–8, https://doi.org/10.1016/j.indcrop.2018.12.060.

[13] V. Somisetti, R. Narayan, R.V.S.N. Kothapalli, Multifunctional polyurethane coatings derived from phosphated cardanol and undecylenic acid based polyols, Prog. Org. Coat. 134 (2019) 91–102, https://doi.org/10.1016/j.porgcoat.2019.04.077.

[14] M.A. Deyab, G. Mele, A.M. Al-Sabagh, E. Bloise, D. Lomonaco, S.E. Mazzetto, C.D.S. Clemente, Synthesis and characteristics of alkyd resin/M-Porphyrins nanocomposite for corrosion protection application, Prog. Org. Coat. 105 (2017) 286–290, https://doi.org/10.1016/j.porgcoat.2017.01.008.

[15] N.L. Jadhav, S.K.C. Sastry, D.V. Pinjari, Energy efficient room temperature synthesis of cardanol-based novolac resin using acoustic cavitation, Ultrason. Sonochem. 42 (2018) 532–540, https://doi.org/10.1016/j.ultsonch.2017.12.001.

[16] M.M. Moreira, L.R.R. da Silva, T.A.D. Mendes, S.L. Santiago, S.E. Mazzetto, D. Lomonaco, V.P. Feitosa, Synthesis and characterization of a new methacrylate monomer derived from the cashew nut shell liquid (CNSL) and its effect on dentinal tubular occlusion, Dent. Mater. 34 (2018), https://doi.org/10.1016/j.dental.2018.04.011.

[17] M. Tubino, J.A. Aricetti, A green potentiometric method for the determination of the iodine number of biodiesel, Fuel 103 (2013) 1158–1163, https://doi.org/10.1016/j.fuel.2012.10.011.

[18] Z. Liu, J. Chen, G. Knothe, X. Nie, J. Jiang, Synthesis of Epoxidized Cardanol and its antioxidative properties for vegetable oils and biodiesel, ACS Sustain. Chem. Eng. 4 (2016) 901–906, https://doi.org/10.1021/acssuschemeng.5b00991.

[19] N. New, C. Dictionary, Standard test methods for determination of gel content and swell ratio of crosslinked ethylene plastics, Annu. B. ASTM Stand. (2005) 1–7, https://doi.org/10.1520/D2765-11.

[20] ASTM:D4541-09, Standard test method for pull-off strength of coatings using portable adhesion, ASTM Int. (2014) 1–16, https://doi.org/10.1520/D4541-09E01.2.

[21] V. Ladmiral, R. Jeannin, K. Fernandes Lizarazu, J. Lai-Kee-Him, P. Bron, P. Lacroix-Desmazes, S. Caillol, Aromatic biobased polymer latex from cardanol, Eur. Polym. J. 93 (2017) 785–794, https://doi.org/10.1016/j.eurpolymj.2017.04.003.

[22] H. Cai, P. Li, G. Sui, Y. Yu, G. Li, X. Yang, S. Ryu, Curing kinetics study of epoxy resin/flexible amine toughness systems by dynamic and isothermal DSC, Thermochim. Acta 473 (2008) 101–105, https://doi.org/10.1016/j.tca.2008.04.012.

[23] K.G. Neoh, E.T. Kang, K.L. Tan, Structural investigations of aromatic amine polymers, J. Phys. Chem. 96 (1992) 6777–6783, https://doi.org/10.1021/j100195a046.

[24] A. Pielesz, A. Wlochowicz, Semiempirical infrared spectra simulations for some aromatic amines of interest for azo dye chemistry, Spectrochim. Acta - Part A Mol. Biomol. Spectrosc. 57 (2001) 2637–2646, https://doi.org/10.1016/S1386-1425(01)00452-8.

[25] E.C.V. Francisco Fraga, E. Rodríguez-Núnez1, J.M. Martínez-Ageitos, Curing kinetics of the epoxy system diglycidyl ether of bisphenol A/isophoronediamine by Fourier transform infrared spectroscopy, Polym. Adv. Technol. 19 (2008) 1623–1628, https://doi.org/10.1002/pat.1178.

[26] R. Liu, X. Zhang, J. Zhu, X. Liu, Z. Wang, J. Yan, UV-curable coatings from multi-armed cardanol-based acrylate oligomers, ACS Sustain. Chem. Eng. 3 (2015) 1313–1320, https://doi.org/10.1021/acssuschemeng.5b00029.

[27] S. Kanehashi, K. Yokoyama, R. Masuda, T. Kidesaki, K. Nagai, T. Miyakoshi, Preparation and characterization of cardanol-based epoxy resin for coating at room temperature curing, J. Appl. Polym. Sci. 130 (2013) 2468–2478, https://doi.org/10.1002/app.39382.

[28] K. Wazarkar, M. Kathalewar, A. Sabnis, Anticorrosive and insulating properties of cardanol based anhydride curing agent for epoxy coatings, React. Funct. Polym. 122 (2018) 148–157, https://doi.org/10.1016/j.reactfunctpolym.2017.11.015.

[29] A. Amirudin, D. Thieny, Application of electrochemical impedance spectroscopy to study the degradation of polymer-coated metals, Prog. Org. Coat. 26 (1995) 1–28, https://doi.org/10.1016/0300-9440(95)00581-1.

[30] K. Wazarkar, A.S. Sabnis, Phenalkamine curing agents for epoxy resin: characterization and structure property relationship, Pigment Resin Technol. 47 (2018) 281–289, https://doi.org/10.1108/PRT-08-2017-0071.

[31] C. Yi, P. Rostron, N. Vahdati, E. Gunister, A. Alfantazi, Curing kinetics and mechanical properties of epoxy based coatings: the influence of added solvent, Prog. Org. Coat. 124 (2018) 165–174, https://doi.org/10.1016/j.porgcoat.2018.08.009.